NATURAL CONVECTION IN CONCENTRIC/ECCENTRIC CYLINDERS EFFECTS OF THE MESH SKEWNESS

C.R. MALISKA and A.F.C. SILVA
MECHANICAL ENGINEERING DEPARTMENT
P.O. BOX 476 - FLORIANOPOLIS -SC
BRAZIL

ABSTRACT

The use of nonorthogonal boundary-fitted coordinates has become,nowadays,a general practice in the solution of fluid flow and heat transfer problems. The generality and the flexibility that its use renders to the model is well known. Despite the tremendous advances that were made in the development of new numerical models involving generalized coordinates, not too much effort has been devoted to the investigation of the influence of highly skewed meshes upon the accuracy of the solution.Fundamental works dealing with truncation errors in nonorthogonal meshes are reported in [1] and [2]. Specific details of the influence of the nonorthogonality in engineering problems are, however, rarely reported.

In this paper it is analyzed the influence of the grid configuration upon the numerical solution of the natural convection problem between concentric and eccentric cylinders placed in the horizontal position. To reach the goal well chosen grids with different characteristics are used in order to have insight into the errors introduced by the mesh skewness. The results are readly extended to other situations.

For the eccentric case the bipolar coordinate system is used to obtain the orthogonal discretization for comparison. The solution for Rayleigh number equal to zero is also obtained for this case, and compared with the analytical solution.

1.INTRODUCTION

It has been reported in [2][3] that the use of highly skewed grids(up to 45 inclination between coordinate lines) does not introduce intolerable errors in the numerical solution. The same findings are reported in [4], in the solution of the fully developed laminar flow in cusped corners when global values are compared. Those results and the grid used are also reported here,for completeness, in Figs.1 and 2. Inspecting these results one can see that there are minor discrepancies in the local values of the equivalent conductivity in the regions where the grid is highly

nonorthogonal,near the cusped corner.

In a recent paper [5], the authors, solving the natural convection problem between concentric cylinders,using a nonorthogonal grid covering the whole domain, as shown in Fig.3b, again have found that the global values of the Nusselt number are in excellent agreement with the solution obtained with a orthogonal grid.The local values, however, did not show the expected symmetry with respect to the vertical axis, as can be

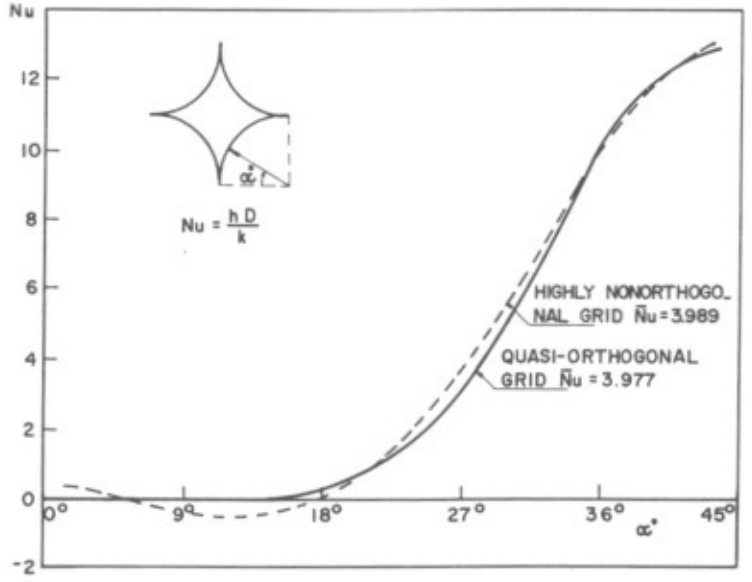

Fig. 1 - Nusselt number for the cusped duct

observed in Fig.4. Two reasons for this unsymmetry were cogitaded : the nonorthogonality involved, and numerical diffusion. The numerical diffusion was avoided in this work solving the problem for a condition where it is possible to use central differencing for all grid points. Therefore, the remainder of the paper will investigate nonorthogonal effects. In this problem the symmetry boundary condition was not used with the purpose of investigating the symmetry of the temperature field.

It does not make sense, of course, to solve the natural convection problem between concentric cylinders, where the physics of the problem shows the existence of a symmetric field, using the grid depicted in Fig. 3(b). The problem solved in this way is, in the other hand, an excellent test for better understanding the influences of the grid nonorthogonality upon the numerical solution.

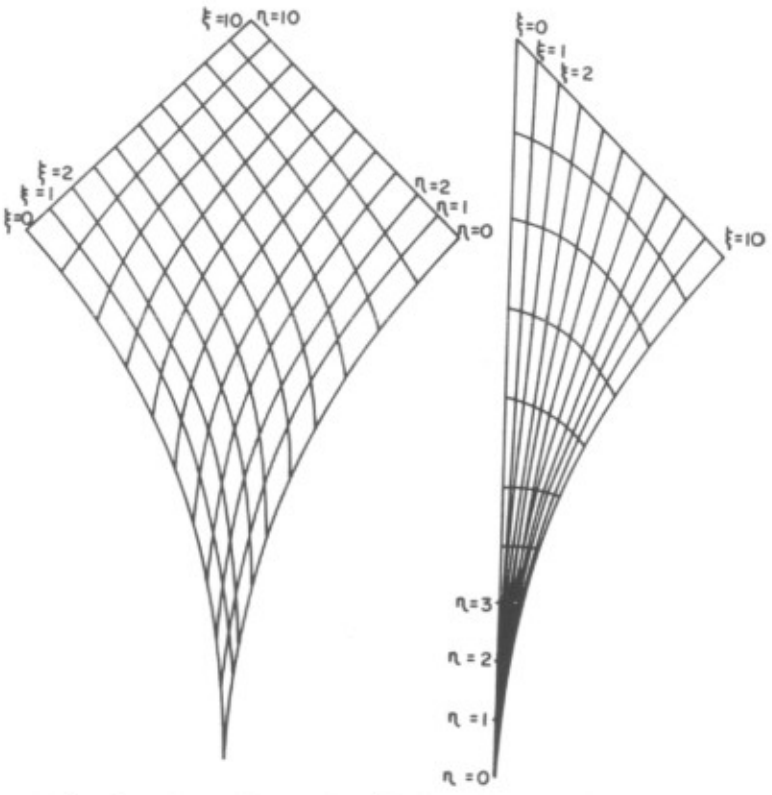

Fig. 2 - Nonorthogonal grid for the cusped duct

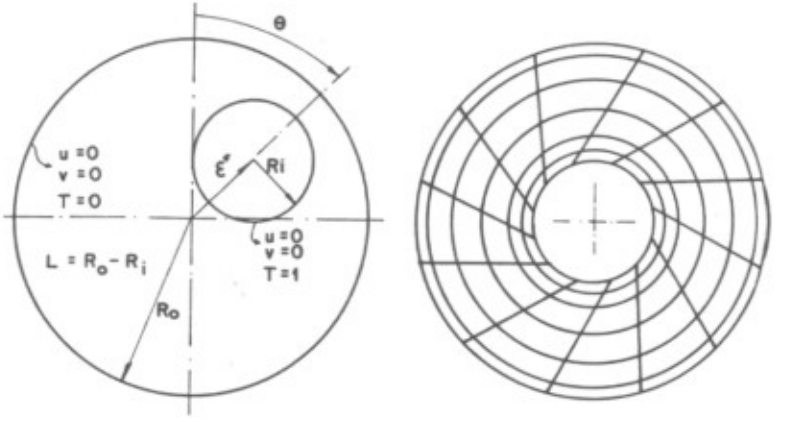

Fig. 3 - a) nomenclature, b) nonorthogonal grid

2. GOVERNING EQUATIONS AND SOLUTION PROCEDURE

The numerical model adopted in this work, except for minor changes, is fully described in [6] and [7] and so, no details will be given here.

For the purpose of this work the natural convection problem between concentric and eccentric cylinders are solved numerically using a two-dimensional model written in generalized coordinates (ξ, η). Using the Boussinesq approximation the governing equations represented by the variable, ϕ are

$$\frac{\rho}{J}\frac{\partial\phi}{\partial t} + \rho\frac{\partial}{\partial\xi}(U\phi) + \rho\frac{\partial}{\partial\eta}(V\phi) + \hat{P}^{\phi} + \hat{C}^{\phi} = \frac{\partial}{\partial\xi}(C_1\frac{\partial\phi}{\partial\xi} + C_2\frac{\partial\phi}{\partial\eta}) + \frac{\partial}{\partial\eta}(C_3\frac{\partial\phi}{\partial\eta} + C_2\frac{\partial\phi}{\partial\xi}) \quad (1)$$

where

$$U = y_\eta u - x_\eta v \qquad V = x_\xi v - y_\xi u \qquad J = (x_\xi y_\eta - x_\eta y_\xi)^{-1} \quad (2)$$

$$C_1 = \Gamma^{\phi} J\alpha \qquad C_2 = -\Gamma^{\phi} J\beta \qquad C_3 = \Gamma^{\phi} J\gamma \quad (3)$$

$$\alpha = x_\eta^2 + y_\eta^2 \qquad \beta = x_\xi x_\eta + y_\xi y_\eta \qquad \gamma = x_\xi^2 + y_\xi^2 \quad (4)$$

and the terms $\hat{P}$ e $\hat{C}$ are given by

$$\hat{P}^u = \frac{\partial P}{\partial\xi}\frac{\partial y}{\partial\eta} - \frac{\partial P}{\partial\eta}\frac{\partial y}{\partial\xi} \qquad \hat{P}^v = \frac{\partial P}{\partial\eta}\frac{\partial x}{\partial\xi} - \frac{\partial P}{\partial\xi}\frac{\partial x}{\partial\eta} \qquad \hat{P}^T = 0 \quad (5)$$

$$\hat{C}^u = 0 \qquad \hat{C}^v = \rho g\beta^*(T - T_{ref})/J \qquad \hat{C}^T = 0 \quad (6)$$

where U and V are the contravariant velocity components and Γ^{ϕ} is the density times the appropriate diffusion coefficient for each variable. The above equations is integrated over space and time to obtain the set of algebraic equations.The extra equation for pressure, to solve the strong coupling between velocity and pressure, is obtained using the PRIME Method [8],which solves the momentum equations formed for the contravariant velocity components [8]. The system of equations are solved in a segregated manner using the MSI - Modified Strongly Implicit Procedure [9] using a 9 points stencil, when only half of the domain is used, and the S.O.R.

technique when the whole domain is employed. Both, temperature and pressure involve nine points in each algebraic equation.

As mentioned, no upwinding is used for all the results reported here.

3. NUMERICAL RESULTS

3.1- Concentric Case

The main concern of this work is to investigate the reasons for obtaining the unsymmetric behaviour of the equivalent conductivity shown in Fig. 4.

As pointed out, the grid employed is shown in Fig.3 (b), where it can be seen that it is not symmetric with respect to the vertical axis. For a symmetric grid the solution must be also symmetric, for any grid size. For the grid independent solution the temperature field and its corresponding equivalent conductivity must be also symmetric, if the numerical model is to work properly.

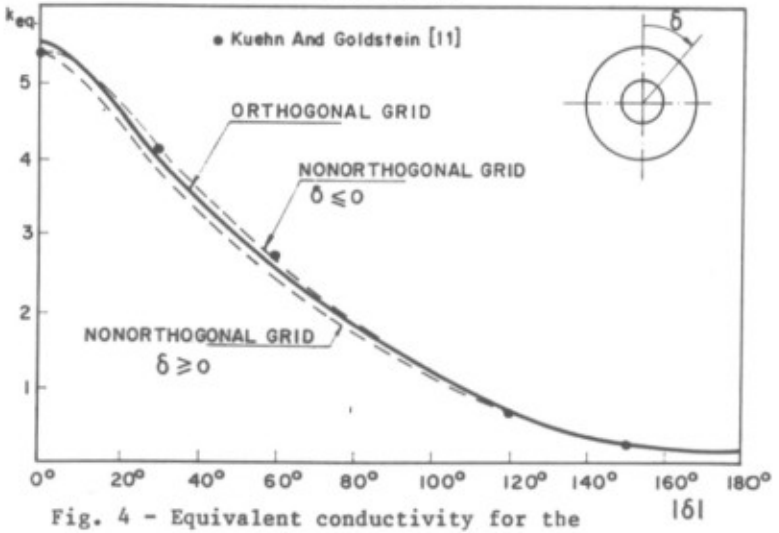

Fig. 4 - Equivalent conductivity for the concentric case

[6]

For better understanding why the heat transfer coefficient is not symmetric for a coarse grid consider Fig. 5, where it is shown the temperatures involved in the calculation of the normal derivatives at the points A and A'. The expression for the normal derivative to a η line is

$$\frac{\partial T}{\partial n} = J\gamma^{\frac{1}{2}}\frac{\partial T}{\partial\eta} - J\gamma^{-\frac{1}{2}}\beta\frac{\partial T}{\partial\xi} \quad (7)$$

Since $\partial T/\partial\xi$ is zero for the the T=1 isothermal wall the normal derivative reduces to

$$\frac{\partial T}{\partial n} = J\gamma^{\frac{1}{2}} \frac{\partial T}{\partial \eta} \qquad (8)$$

It can be realized, with the help of Fig.5, that there is no way to obtain the same derivatives at the points A and A', because the points B and C and B' and C' are not symmetric to each other, even if the temperature field were symmetric. The normal derivative will tend to become equal only for a very fine grid near the boundary. Therefore, this unsymmetry is a consequence of the grid configuration. In Fig. 6 it is shown the isotherms for this case, where , indeed, one can detect a slightly nonsymmetric temperature field. How this unsymmetry behaves with the grid refinement is now addressed.

In the following tables and figures the results obtained in the solution of the concentric case, using different grid sizes and different grid configurations are reported. Table I shows the equivalent conductivity calculated at the external cylinder , for several situations, as explained, according to

$$k_{eq} = \frac{q}{q_{cond}} \qquad (9)$$

where q is the local heat flux for the geometry under consideration and q_{cond} is the local heat flux for the pure conduction problem for the concentric cylinder, which is a constant value.

The results shown in lines d and e are the ones reported in Fig.4, obtained with a 10x72 nonorthogonal mesh. It is important to recall here that for the concentric case all nonorthogonal grids are nonsymmetric with respect to the vertical axis. Lines f and g bring to the reader the results for the same problem obtained with a 18x60 grid while lines h and i report the results for a 26x60 mesh.

Fig. 7 reports the percent error between the results calculated at both sides of the calculation domain ($\delta < 0$ and $\delta > 0$), with respect to the average value between these values. This error is a measure of the nonsymmetry of the equivalent conductivity distribution. It is clear that using finer grids in the radial direction, the symmetry is considerably improved, what suggests that this nonsymmetry, which is absent for a symmetric grid with any size, in this case is a grid dependent parameter.

The findings reported above are, however, detected only by the "sensors" used by the numerical analyst interested in

better understanding the behaviour of the numerical models. In the point of view of the solution quality, it can be seen with the aid of Table I that the maximum percent error between the local equivalent conductivity number, compared with that obtained with an orthogonal grid with the same grid size, is of the order of less than 1.5%, which means that the results using the nonorthogonal model are very good. Indeed, the average equivalent conductivity , comparing orthogonal and nonorthogonal grids with 18x60 and 26x60 grid point is exactly the same up to 3 sigficant digits.

TABLE I

	0^0	30^0	60^0	90^0	120^0	150^0	180^0	$\bar{K}_{eq}$
a	5.538	4.052	2.606	1.542	0.722	0.265	0.150	2.000
b	5.378	3.954	2.614	1.551	0.720	0.271	0.155	1.976
c	5.323	3.925	2.607	1.537	0.715	0.273	0.157	1.963
d	5.416	3.843	2.450	1.435	0.687	0.275	0.148	1.977
e	5.416	4.186	2.706	1.606	0.740	0.247	0.148	
f	5.335	3.919	2.573	1.529	0.712	0.269	0.155	1.975
g	5.335	3.987	2.651	1.581	0.737	0.273	0.155	
h	5.275	3.934	2.585	1.524	0.708	0.272	0.157	1.962
i	5.275	3.926	2.626	1.555	0.725	0.275	0.157	
j	5.35	4.10	2.72	1.54	0.68	0.26	0.14	2.005

a - orthogonal grid 10x72
b - orthogonal grid 18x60
c - orthogonal grid 26x60
d - nonorthogonal grid 10x72 ($\delta > 0$)
e - nonorthogonal grid 10x72 ($\delta < 0$)
f - nonorthogonal grid 18x60 ($\delta > 0$)
g - nonorthogonal grid 18x60 ($\delta < 0$)
h - nonorthogonal grid 26x60 ($\delta > 0$)
i - nonorthogonal grid 26x60 ($\delta < 0$)
j - reference [11]

All cases: Pr=0.70, $Ra=10^6$, Ro/Ri=2.60

Anyway, despite the excellent results obtained with the nonorthogonal model, it is recommended that grid as orthogonal as possible should be used at the boundaries [1].

Finally, it is important to point out that for checking purposes, in the orthogonal case the problem was also solved using only half of the domain. As expected, no differences in the heat tranfer coefficients or in the flow pattern were observed for all computations carried out, with Rayleigh number varying up to 10^6 . In [10] it is reported that using the whole domain to obtain the solution the flow pattern was different from the one obtained using the symmetry boundary condition, and a counterclockwise convection loop appeared in the top portion of the enclosure.

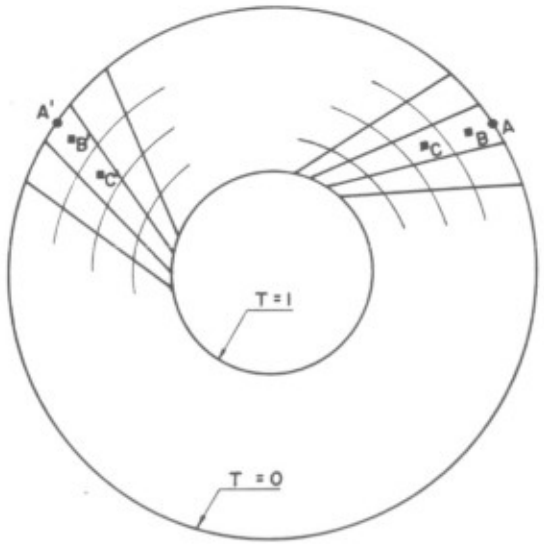

Fig. 5 - Nonorthogonality at the boundaries

Fig. 6 - Isotherms for the concentric case

3.2- Eccentric case

The eccentric case offers even more possibilities for assesment of the numerical model. It is possible, with this geometry, to solve the problem using nonorthogonal symmetric grids, as well as to generate orthogonal grids using the bipolar coordinate system. The problem is solved for the geometry shown in Fig. 8, with ε_r=0.625 and L/D_i = 0.8.

The same Rayleigh and Prandtl numbers of the previous case is used, and the problem is solved for the grids depicted in Figs. 8, 9 and 10. The discretization shown in Fig. 8 is orthogonal,obtained using the bipolar coordinate system, while the ones shown in Figs. 9 and 10 are nonorthogonal. All of the grids exhibit symmetry with respect to the vertical axis. The grids shown in Fig. 8 and 9 are constructed for being as similar as possible to each other.

Fig. 11 shows the local equivalent conductivity using the grids just described. The results obtained with the orthogonal grid are plotted in curve 2, while the ones obtained with the nonorthogonal grid similar to the orthogonal are depicted in curve 3. The maximum percent error between the local values are of the order of 1.5 %. For the other nonorthogonal grid the error is a bit higher, increasing up to 3.5 %. These local values are not tabulated because they are calculated for different angles and the comparison can not be made number by number.

What it is important to point out here is that the nonorthogonality degree of the grids shown in Fig. 9 and 10 are practically the same. Therefore, the higher errors observed for curve 3 are due to the poor grid resolution in the top part of the enclosure, exactly the region where a fine grid is most needed due to the physics of the phenomenon.

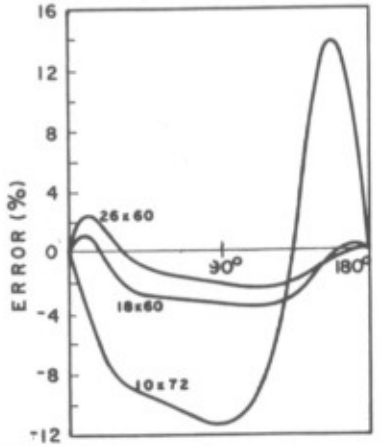

Fig. 7 - Percent error

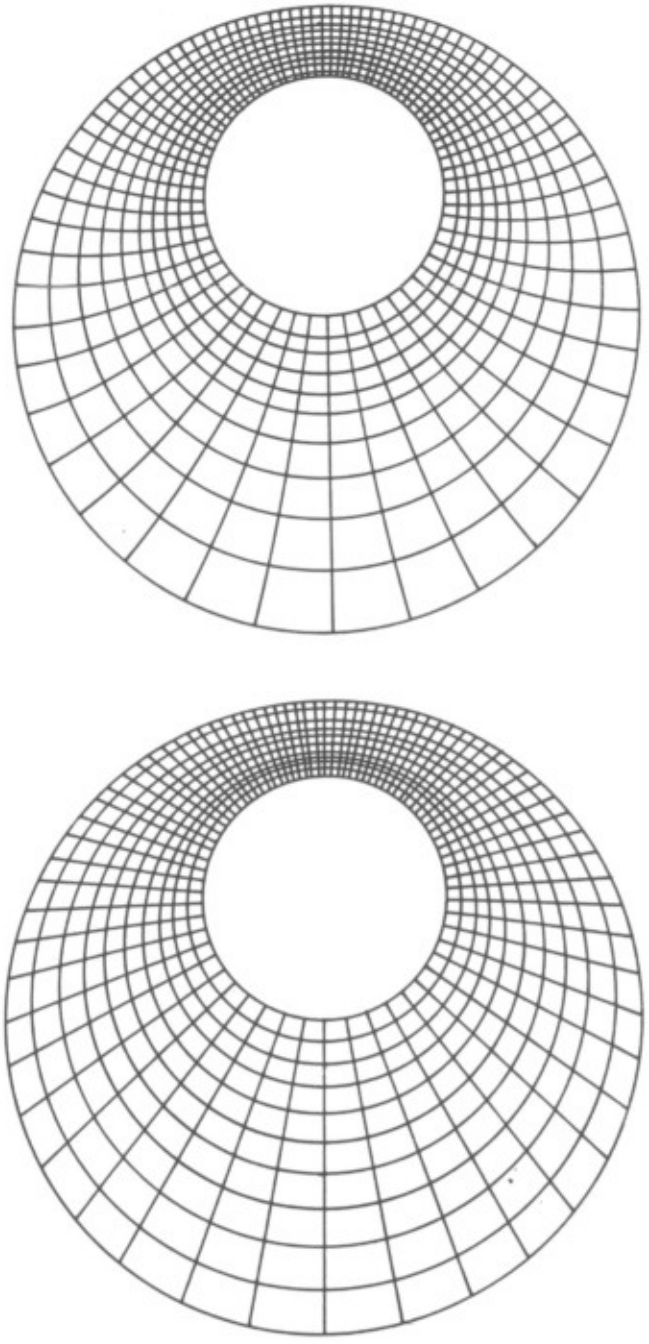

Fig. 8 and 9 - Orthogonal and Nonorthogonal Grids

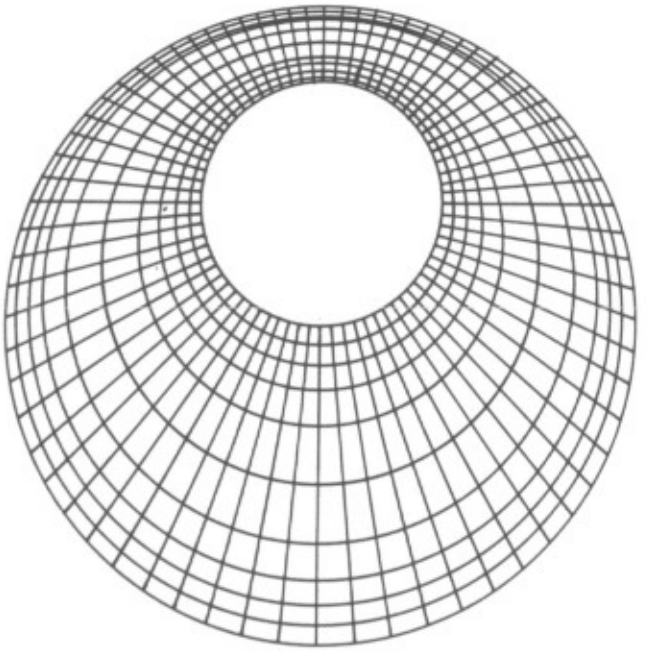

Fig. 10 - Nonorthogonal discretization

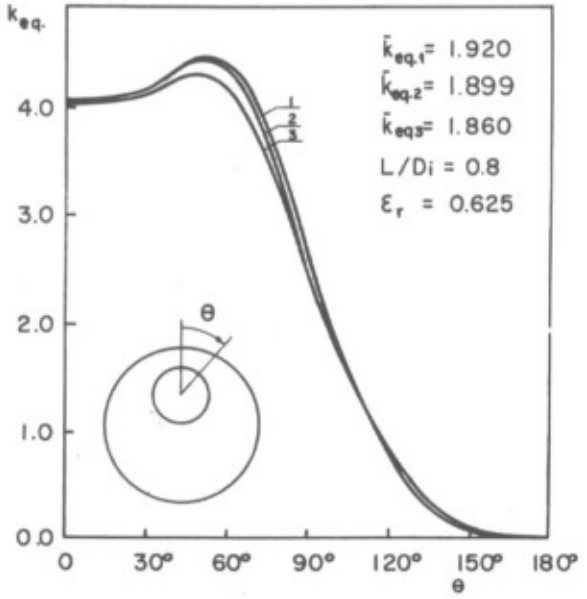

Fig. 11 - Local equivalent conductivity

These findings confirm, again, that to relax the orthogonality to a certain extent does not introduce errors, specially if global values are required. Of most importance is to have an adequate grid refinement in the regions where it is needed, as demonstrated.

To finalize, Table II shows the global equivalent conductibility, defined as before,for the pure conduction problem in the eccentric cylinder. The tabulated order is analytical, grid of Fig. 9,grid of Fig. 10 and orthogonal.As can be seen the results agree very well with the analytical results obtained solving the pure conduction problem in bipolar coordinates. As a final remark it is important to be noted that the grids used for the excentric case are not fine enough in the radial direction. For the purpose of this comparison it was not necessary to increase the number of grid points.

TABLE II

$\bar{k}_{eq}$			
1.2632	1.264	1.268	1.263

4. CONCLUSIONS

The natural convection problem in concentric and eccentric cylinders was solved using a boundary fitted method with the aim of investigating the effects of the grid nonorthogonality upon the numerical solution. It was demonstrated that the errors observed in the local values of the equivalent conductibility are so small that the solution quality is not damaged. Despite this fact it was also concluded that it is always beneficial to have, as nearly as possible, orthogonal discretization at the boundaries.

5. REFERENCES

[1]. J.F. Thòmpson and C.W. Mastin, "Order of Difference Expressions in Curvilinear Coordinates Systems",in Advances in Grid Generation, ASME FED vol 5, K.Ghia, U. Ghia , Eds.,1983.

[2]. J.F. Thompson, "Grid Generation Techniques in Computational Fluid Dynamics",AIAA Journal, Vol.22 n.11, pp. 1505-1523,1984.

[3]. M. Braaten and W. Shyy, " A Study of Recirculating Flow Computation Usign Body-Fitted Coordinates: Consistency Aspects and Mesh Skewness", Num. Heat TRansfer, vol. 9, pp.559-574,

1986.

[4]. C.R. Maliska and A.F.C. Silva, " Local Effects of Highly Nonorthogonal Grids in the Solution of Heat Transfer Problems in Cusped Corners", Numerical Grid Generation in Computational Fluid Dynamics, J. Hauser and C. Taylor, Eds. pp.679-690, Pineridge Press, 1986.

[5]. A.F.C. Silva and C.R. Maliska, " Previsao Numerica da Transferencia de Calor por Conveccao Natural em Cavidades Duplamente Conexas Arbitrarias", II Latin American Congress of Heat and Mass Transfer, pp. 74-85, vol.I, May 1986.

[6]. C.R. Maliska and G.D. Raithby,"A Method for Computing Three-Dimensional Flows using Nonorthogonal Boundary-Fitted Coordinates", Int. J. Num. Meth. in Fluids, Vol. 4, pp.519-537,1984.

[7]. C.R. Maliska and G.D. Raithby, " Calculating Three-Dimensional Flows using Nonorthogonal Grids", Numerical Methods in Laminar and Turbulent Flow, C. Taylor, J.A. Johnson and W.R. Smith, pp. 656-666, Pineridge Press, 1983.

[8]. C.R. Maliska, " A Solution Method for Three-Dimensional Parabolic Fluid Flow Problems in Nonorthogonal Coordinates",Ph.D. Thesis, University of Waterloo, Canada, 1981.

[9]. G.E. Schneider and M.Zedan, " A Modified Strongly Implicit Procedure for the Numerical Solution of Field Problems", Num. Heat Transfer, vol.4, pp.1-19, 1981.

[10]. U. Projhan, H. Rieger and H. Beer, " Numerical Analysis of Laminar Natural Convection Between Concentric and Eccentric Cylinders", Num. Heat Transfer, vol.4 pp 131, 1981.